Fast isotope mixing in Ion Temperature Gradient driven turbulence

J. Citrin[1], C. Bourdelle[2], Y. Camenen[3], M. Marin[1], F.J. Casson[4], F. Koechl[5], M. Maslov[4] and JET Contributors[6]

[1] *DIFFER - Dutch Institute for Fundamental Energy Research, Eindhoven, the Netherlands*

[2] *CEA, IRFM, F-13108 Saint-Paul-lez-Durance, France*

[3] *CNRS, Aix-Marseille Univ., PIIM UMR7345, Marseille, France*

[4] *CCFE, Culham Science Centre, Abingdon, Oxon, OX14 3DB, UK*

[5] *ÖAW/ATI, Atominstitut, TU Wien, 1020 Vienna, Austria*

[6] *See the author list of X. Litaudon et al 2017 Nucl. Fusion 57 102001*

The degree of density peaking in tokamaks depends strongly on turbulence regime, which impacts the convective velocity direction [1, 2]. In a multi-ion plasma, additional complexity is introduced where ion profiles may respond to transients at a timescale independently from the electrons. Understanding these dynamics is key for predicting DT fuelling and He ash removal in fusion reactors. Experimental evidence for fast isotope mixing has been observed in trace tritium (T) experiments [3, 4]. Recent JET mixed isotope (H/D) experiments has shown density peaking of H and D isotopes independent from the H and D core sources, leading to an interpretation of $D_{i(H,D)} \gg D_e$ [5]. This is consistent with previous analysis of He transport [6, 7], where a large $D_{He} \sim \chi_{eff}$ was observed.

We show that the diffusive and convective ion coefficients are indeed predicted to be significantly larger than those of electrons for ion-temperature-gradient (ITG) driven turbulence. In this regime, for multiple-ion plasmas, the ion density profiles are then insensitive to the ion particle sources, seen from integration of the ion particle transport equation in stationary state:

$$-\frac{1}{n_i}\frac{\partial n_i}{\partial r} = -\frac{V_i}{D_i} + \frac{1}{V'}\int_0^r V' \frac{S_i}{n_i D_i}\,\mathrm{d}r \tag{1}$$

where S_i is the source term, V' the radial derivative of the plasma volume, D_i the ion diffusivity, and V_i the ion convection. If $D_i \gg S_i/n_i$, then the source has a negligible impact on the density peaking. These statements are supported through nonlinear simulations, analytical derivations and quasilinear transport models in fixed gradient standalone mode and used within integrated modelling. The results are further expanded in Ref. [8].

In a simplified analytic quasilinear gyrokinetic limit, detailed in Ref. [8], it can be shown that large D_i/D_e and $|V_i|/|V_e|$ is a consequence of wave-particle resonances for modes propagating in the ion diamagnetic direction, i.e. ITG modes. The inverse is the case for Trapped Electron Modes (TEM). The mechanism is similar to that which leads to heat flux ratios $Q_i/Q_e >$ for

ITG and $Q_e/Q_i > 1$ for TEM. However, the significant convective terms in particle transport can maintain ambipolarity in spite of the disparity in transport coefficient magnitudes. From the decomposition of the particle flux: $\Gamma = -D\frac{dn}{dr} + Vn$, ambipolarity (e.g. $\Gamma_i = \Gamma_e$ for a 2-species plasmas) can be satisfied by:

$$-D_i \frac{dn_i}{dr} + V_i n_i = -D_e \frac{dn_e}{dr} + V_e n_e \tag{2}$$

through a significant compensation between outward ion diffusion and inward ion convection. For a multi-ion plasma, where ambipolarity means $\sum_i Z_i \Gamma_i = \Gamma_e$, then in transient phases the large D_i and V_i can lead to fast ion mixing, as observed in mixed isotope experiments.

The clear trends from these expectations from quasilinear analytics are recovered by quasilinear and nonlinear gyrokinetic calculations with QuaLiKiz [9, 10] and GKW [11] respectively. This is seen in figure 1, where the particle diffusivity from GKW nonlinear runs for ITG and TEM regimes around the GA-Standard case (see table 1 for input parameters), are compared with a QuaLiKiz ion temperature gradient scan.

The diffusivity ratios correspond to $D_i/D_e > 1$ for the ITG case, and $D_i/D_e < 1$ for the TEM case, in line with the analytical expectations. Note also the agreement between GKW nonlinear and QuaLiKiz quasilinear predictions for the diffusivity ratios. Similar results are obtained for the convective terms, omitted for brevity.

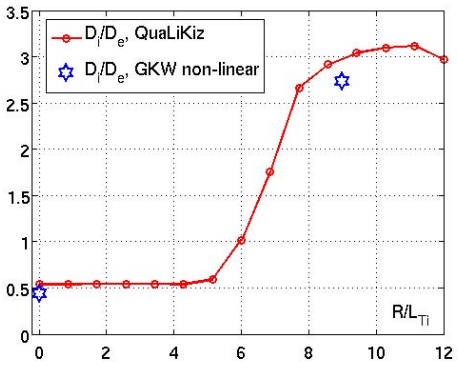

Figure 1: *Ratio of ion to electron particle diffusivities versus R/L_{T_i} (other parameters from GA standard case, see Table 1). The red circles are for QuaLiKiz ratios and the blue stars for nonlinear-GKW ratios.*

The implications of this trend are illustrated through analysis of multiple-isotope transport dynamics within an integrated modelling framework, applying JETTO [12, 13] coupled to QuaLiKiz for turbulent transport predictions. The starting point was the JET baseline H mode pulse #87412, previously analysed using JETTO-QuaLiKiz with good quantitative agreement [10]. A multiple-isotope scenario was then artificially imposed on the simulations, introducing an H species in the D pulse with $n_H = n_D$ in the $\rho = 0.85 - 1.0$ region, where ρ is the normalised toroidal flux coordinate. The electron density profile n_e was kept as in the original discharge. The PENCIL NBI source calculations are peaked off-axis due to high n_e. To simulate various regimes, the sources were artificially modified in the various cases, as described below. QuaLiKiz was applied in

Case	$\frac{r}{R}$	q	$\hat{s}$	$\frac{R}{L_{T_e}}$	$\frac{R}{L_{n_e}}$	$\frac{R}{L_{T_i}}$	$\frac{R}{L_{n_i}}$	$\frac{T_e}{T_i}$
ITG	0.1667	2	1	9	3	9	3	1
TEM	0.1667	2	1	9	3	0	3	1

Table 1: Summary of the input parameters for the ITG and TEM cases.

the region $0.15 < \rho < 0.85$, with boundary conditions from measurements. Multiple energy confinement times were run for full convergence.

Following reaching stationary state for T_i, T_e and n_e with a 50-50 H-D concentration and a D particle source, the NBI particle source was artificially switched to pure D, and the simulation restarted until re-reaching stationary state. The D profile evolution in the post-switch transient phase can be seen in Fig. 2 (left panel) at $\rho = 0.6$. The final density profiles for D, H and electrons are visible in Fig. 2 (central panel). The D relaxation timescale was determined to be $\tau = 60\,\text{ms}$ following an exponential fit, i.e. faster than the energy confinement time $\tau_E \approx 100\ ms$.

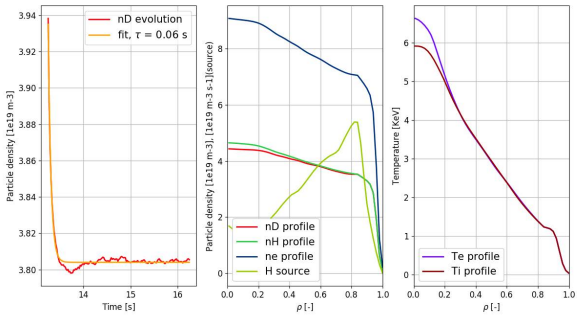

Figure 2: *Evolution of the D density profile at $\rho = 0.6$ following a switch of particle source from D to H (left panel). The τ relaxation timescale is from an exponential fit. The central panel shows the final relaxed density profiles in presence of a H source, while the right panel shows the relaxed temperature profiles, at 16 s*

Note that both H and D profiles are peaked, in spite of only D particle source. This indicates that both D and H profiles are controlled by the large D_i and an inward V_i.

In the second case, starting from the same initial profiles, all particle sources were turned off to identify the timescale of electron particle transport. The results are shown in Fig. 3, with the left panel corresponding to the decay of n_e, n_H and n_D at $\rho = 0.6$, and the final relaxed density profiles shown in the central panel. The decay of D, H and n_e coincide, since the evolving electrons control the isotope transport. As expected from the differing ion and electron transport coefficients, this timescale is around 5 times slower than in the isotope mixing case, with $\tau = 0.28\,\text{s}$ and slower than the energy confinement time. The final electron density profile, without source, is slightly flatter than the initial one with an off-axis source. Even though JETTO only evolves the ions (and sets n_e through quasineutrality), the slower ion transport in this case is caused by the time-dependent impact of the evolving R/L_{ne} on the ion transport coefficients.

In summary, through a comprehensive approach involving quasilinear, nonlinear, and integrated source-driven modelling, we have demonstrated that ion particle transport coefficients differ significantly from electron particle transport coefficients while respecting ambipolar fluxes. This leads to a separation between electron and ion particle transport timescales, with fast isotope mixing, and a low dependence of isotope peaking on isotope sources. The isotope profile thus depends on the electron peaking and the edge isotope boundary conditions.

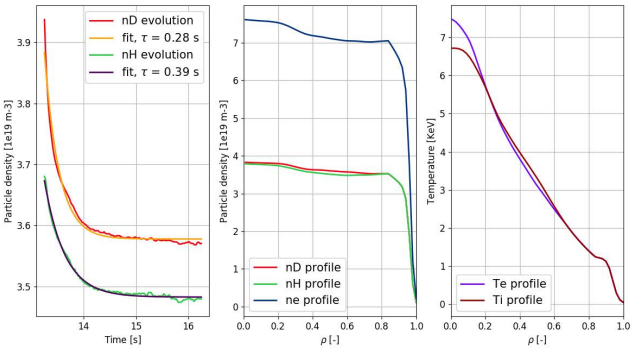

Figure 3: *Evolution of n_e and n_D at $\rho = 0.6$ after turning off all particle sources (left panel). The final relaxed density profiles are shown in the central panel, the final temperature profiles are shown in the right panel, at 16 s.*

Our findings are consistent with numerous experimental observations, e.g. similar H and D density profiles in JET-ILW in presence of core D source [5]. Presently, QuaLiKiz-JETTO is being applied for these specific experiments with quantitative agreement [14], further supporting the veracity and relevance of large ion transport coefficients to explain this behaviour. In future work, ITER scenarios will then be addressed focusing on isotope mixing, He ash transport, edge fuelling, and impurity contamination in H, He and DT scenarios.

Acknowledgments.– This work has been carried out within the framework of the EUROfusion Consortium and has received funding from the Euratom research and training programme 2014-2018 under grant agreement No 633053. The views and opinions expressed herein do not necessarily reflect those of the European Commission.

References

[1] C. Angioni *et al.,* Plasma Phys. Control. Fusion **51** 124017 (2009).
[2] E. Fable and C. Angioni Plasma Phys. Control. Fusion **52** 015007 (2010).
[3] P. C. Efthimion *et al.,* 1995 Phys. Rev. Lett. 75 1.
[4] K-D Zastrow *et al.* 2004 Plasma Phys. Control. Fusion **46** B255.
[5] M. Maslov *et al.* 2018 Nucl. Fusion **58** 076022.
[6] M. R. Wade *et al.,* 1995 Phys. Plasmas ,**2** 2357.
[7] C. Angioni *et al.,* Nucl. Fusion **49** 055013 (2009).
[8] C. Bourdelle *et al.,* accepted to Nucl. Fusion.
[9] C. Bourdelle *et al.* 2007 Phys. Plasmas **14** 112501.
[10] J. Citrin *et al.* 2017 Plasma Phys. Control. Fusion **59** 124005.
[11] A.G. Peeters *et al.* 2009 Computer Physics Communications **180** 2650.
[12] G. Cenacchi, A. Taroni, JETTO: A free-boundary plasma transport code, JET-IR (1988).
[13] M. Romanelli *et al.* 2014 Plasma and Fusion Research Volume 9, 3403023.
[14] M. Marin *et al.,* EPS Prague 2018, O2.102.